BJPS

Brazilian Journal of Pharmaceutical Sciences

http://dx.doi.org/10.1590/s2175-97902025e24261

Article

Formulation of anise seeds essential oil nanoemulsion stabilized by chitosan/ polysorbate using full factorial design: oxidative stability and antimicrobial activity

Issaadi Halima Meriem[1]*, Boudjema Nouara[2], Sahraoui Naima[2], Nait Bachir Yacine[2]

[1]Laboratory of Chromatography, Department of Organic Chemistry, Faculty of Chemistry, University of Sciences and Technology Houari Boumediene (USTHB), Algiers, Algeria, [2]Department of Biology, Faculty of Natural and Life Sciences, University Saad Dahlab, Blida, Algeria

The purpose of the present study is to prepare anise (*Pimpinella anisum L.*) seeds essential oil nanoemulsions using a full factorial experimental design. Tween 80 content (0.5-1%, X1), chitosan content (0.5-1%, X2), irradiation time (60-80s, X3) and ultrasonic amplitude (35-40%, X4) were selected as independent variables whereas mean droplet size (nm, Y1) and polydispersity index (Y2) as dependent variables. The accuracy of the generated mathematical models was evaluated using multiple linear regression. Moreover, oxidative stability during storage and antimicrobial activity of free and nanoemulsion anise seeds essential oil were evaluated. Experimental selected conditions were 80s irradiation time with 40% ultrasonic amplitude, stabilized with 0.5% chitosan and 1% polysorbate 80. The obtained results indicated the perfect nanodispersion of essential oil in water. Lastly, oxidative stability determined by the primary and secondary oxidation products and antimicrobial activity of anise seeds essential oil against various Gram+ and Gram- microorganisms were significantly increased after the nanodispersion. Hence, this study concludes that the mathematically modelled formulation of anise seed essential oil nanoemulsion systems, stabilized by polysorbate 80 and chitosan, exhibited significantly improved oxidative stability and antibacterial activity compared to the free essential oil.

Keywords: Anise seeds essential oil. Nanoemulsion. Ultrasonication. Full factorial design. Oxidative stability. Antimicrobial activity.

INTRODUCTION

The growing focus on employing micro- and nanosystems within pharmaceutical, food, and cosmetic sectors has been driven by their numerous benefits compared to conventional emulsions (Nait Bachir, Nait Bachir, Hadj-Ziane-Zafour, 2018; Nait Bachir, Zafour, Medjkane, 2018; Nait Bachir *et al*., 2017). Nanoemulsions are a particular category of emulsions that have a unique appearance, i.e they are transparent or translucent and have an intense bluish shine. Nanoemulsions, characterized by the small size of their droplets, exhibit physical resistance thanks to their ability to flocculate, sediment or coalesce (Wooster, Golding, Sanguansri, 2008; Nait Bachir *et al*., 2022). The stable nature of the nanodroplets in nanoemulsions makes them suitable for use in a wide range of applications, unlike the poor stability and large size of the materials when in their microemulsion state. When compared to traditional delivery systems, nanoemulsions carriers' present improved biocompatibility and better penetration of the targeted active site and particularly of microbial walls, causing microbe mortality and thus an inhanced antimicrobial efficency (Canselier *et al*., 2002).

The formation of nanoemulsions is a non-spontaneous phenomenon and thus requires high- or low-energy emulsification to produce the droplets (Gumiero, Da Rocha Filho, 2012). Concerning high-energy emulsification methods, large mechanical energy is generated by the use of high pressure homogenizers,

***Correspondence:** H. M. Issaadi, Laboratory of Chromatography, Department of Applied Organic Chemistry, Faculty of Chemistry, University of Sciences and Technology Houari Boumediene (USTHB), BP 32 Bab Ezzouar, 16111, Algiers, Algeria, Phone: +213561060049, E-mail: hmissaadi@usthb.dz, https://orcid.org/0000-0002-7792-3183.

ultrasound, or microfluidizers (Sakulku *et al*., 2009; Puglia *et al*., 2010). At the same time, the surfactants play a key role in the formulation and stabilization of nanoemulsions in both droplet breakup and stability of the nanoemulsions due to the reduction of interfacial tension and the resistance to droplet deformation (Leong *et al*., 2009; Slamani *et al*., 2020). The major advantage of such method is that the average volume size of nanoemulsions particles is a function of the formulation composition, which means that nanoemulsions size can be handily customized by formulation design (Shaaban, El-Ghorab, Shibamoto, 2012).

Essential oils have been used in personal care, and pharmaceutical and cosmetics industries as active substances for their fragrance and therapeutic properties for decades and there has seen significant growth in their use in recent years. Anise seeds essential oil (ASEO) have been used in industry as an active substance. In fact, the large spectrum of significant bioactivities of ASEO has already been assessed by several studies, including antibacterial, antiviral, anti-inflammatory, antifungal and antioxidant as well as other miscellaneous activities (Shojaii, Abdollahi Fard, 2012). So far, few ASEO nanoemulsions have been successfully developed, displaying enhanced antimicrobial efficacy against a range of pathogens (Abu Ali *et al*., 2021; Ghazy *et al*., 2021) and insecticidal and larvicidal efficiency (Hashem *et al*., 2018; Hashem *et al*., 2020; Draz *et al*., 2022).

In the present research work, the aims are: a) to use experimental design in order to screen the ASEO nanoemulsions obtained by ultrasonication technique and stabilized by chitosan/polysorbate 80 surfactants; b) to suggest the mathematical model of this process including four factors: Tween 80 content, chitosan content, irradiation time and ultrasonic amplitude and two responses: polydispersity index and droplet size; c) to evaluate and enhance the oxidative stability of the prepared nanoemulsion; d) to assess the antimicrobial activity and behavior of nanoemulsions against Gram- and Gram+ bacteria.

MATERIAL AND METHODS

Material

ASEO was obtained by hydro-distillation (86.02% trans-anethole, determined by GC/MS). Chitosan was prepared by demineralization, deproteinization, and deacetylation process from crab shell (degree of deacetylation 91%, molecular weight 340,000); Tween 80 was procured from Sigma-Aldrich (USA). All other materials used are of pharmacopoeial grade.

Extraction and characterization of ASEO

Extraction of ASEO by hydro-distillation

The dry anise seeds were purchased from the local market in Algiers - Algeria. Anis seeds essential oil was obtained by hydro-distillation of the powdered dry material according to the British Pharmacopeia Protocol (2003). Briefly, fractions of 40 g vegetal material were submitted to hydro-distillation using a Clevenger-type apparatus (Enava Company, Boumerdes, Algeria) for 3 hours. The resulting essential oil was dried over anhydrous sodium sulphate, filtered, and stored at 4°C until analyses. The essential oil yield was expressed based on dry weight of the vegetal matter.

Characterization of ASEO by GC-MS

The analysis of the essential oil was performed using a Hewlett Packard 6890 gas chromatograph coupled to a 5973A mass spectrometer, equipped with a HP5MS™ fused silica capillary column (30 m × 0.25 mm ID × 0.25 µm film thickness). For GC/MS detection, an electron ionization system was used with ionization energy of 70 eV. Helium was the carrier gas at a flow rate of 0.5 $ml.min^{-1}$. Injector and detector (MS transfer line) temperatures were set to 250 and 280°C respectively. Column temperature was initially at 60°C for 8min, and then increased at a rate of 2°C/min up to 280°C and held at that temperature for 10 min. Samples of 1.0 µl

were injected with a split ratio of (20:1). The retention index (RI) of all the constituents was determined via the Kovats method by co-injection of the samples with a solution containing the homologous series of n-alkanes (C_8-C_{24}) on the HP5MS™ column. Identification of the components was made by visual interpretation, comparing their retention indices and mass spectra with data published in the literature (Adams, 2007) and by matching their recorded mass spectra with reference spectra in the computer library NIST 11 (National Institute of Standards and Technology). The quantification amounted to computing the percentage contribution of each compound to the total amount present.

Formulation of ASEO nanodispersion

For the emulsion process fabrication, a mixture of ASEO was dispersed in bi-distilled water at 5% containing Tween 80 and chitosan, using an Ultra Turrax T25 (IKA, Germany) at 24,000 rpm for 5 min, to form primary emulsion. Afterward, the emulsion was subjected to sonication using a Sonicator (Ultrasonics, USA) at a high frequency of 20 kHz and power output of 750 W. Energy input was given through sonicator probe with a probe diameter of 13 mm which generates strong disruptive forces and reduces droplet size of emulsion. The formulated nanoemulsions were subsequently characterized with Laser Particle Size Analyzer. All nanoemulsion formulations codes with their composition and their sonication parameters are shown in Table I.

TABLE I - Nanoemulsion formulations codes, compositions and ultrasonication parameters

Formulations codes	ASEO content	Tween 80 content	Chitosan content	Irradiation time (seconds)	Ultrasonic amplitude (%)
ND 1	5%	1%	1%	60	40
ND 2	5%	0.5%	1%	60	40
ND 3	5%	1%	0.5%	60	40
ND 4	5%	0.5%	0.5%	60	40
ND 5	5%	1%	1%	80	40
ND 6	5%	0.5%	1%	80	40
ND 7	5%	1%	0.5%	80	40
ND 8	5%	0.5%	0.5%	80	40
ND 9	5%	1%	1%	60	35
ND 10	5%	0.5%	1%	60	35
ND 11	5%	1%	0.5%	60	35
ND 12	5%	0.5%	0.5%	60	35
ND 13	5%	1%	1%	80	35
ND 14	5%	0.5%	1%	80	35
ND 15	5%	1%	0.5%	80	35
ND 16	5%	0.5%	0.5%	80	35

Experimental design

In the present study, a 2^4 factorial design was used with two levels (-1 and +1) and four factors (X1, X2, X3 and X4) which were: Tween 80 content (0.5-1%, X1), chitosan content (0.5-1%, X2), irradiation time (60-80s, X3), and ultrasonic amplitude (35-40%, X4). The two responses were mean droplet size (Y1) and polydispersity index (Y2).

The number of experiments required for this design was calculated following the equation :

$$N=Lv$$

L : the number of levels for the investigation (two in our case),

v : the number of factors (four in our case).

Thus, sixteen independent experiments were carried out to investigate the experimental domain.

The dependence of experimental responses "Y" on the factors were modelled applying the following equation (Box, Hunter, Hunter, 1978):

$$Y = \beta_0 + \sum_{i=1}^{n} \beta_i x_i + \sum_{i=1}^{n} \sum_{j=i+1}^{n} \beta_{ij} x_i x_j + \varepsilon$$

β_0 : the constant term,

βi and βij : the regression coefficients,

ε : the error,

xi and xj : the variables.

The obtained experimental results were analysed with the MODDE Pro 13 software. The accuracy of the mathematical models was evaluated using a summary of the fit. This method includes the goodness of fit R^2, the adjusted R^2, and the goodness of prediction Q^2 where R^2 is an overestimated measure and Q^2 is an underestimated measure of the goodness of fit of the model (Salfinger, Tortorello, 2015).

Determination of ASEO content in nanoemulsions

A 10 g aliquot of each formulation was introduced into a flask containing 100 ml of distilled water. The flask was then placed in a Clevenger-type hydro-distillation extraction system. After one hour of extraction, the essential oil present in the formulation was carefully collected and weighed. The amount of essential oil in the formulation was determined using the following equation:

$$\text{Percentage of essential oil} = \frac{\text{mass of extracted oil}}{10} * 100$$

The determination of the percentage of essential oil present in the formulations was performed in triplicate, and the results are reported as an average along with the standard error.

Laser Particle size analysis

Laser particle size analysis of all nanoemulsion formulations were determined, in triplicate, using Nanotrac ™250 (Microtrac Inc., PA, USA) Instruments, the droplet size distribution was characterized in terms of the mean droplet size and polydispersity index by measuring the backscattered (173°) light through samples diluted 1:100 with bi-distilled water in order to avoid multiple scattering effects within polystyrene cuvettes.

Zeta potential measurement

The zeta potential of ND 7 was determined using Nanotrac Instruments, the measurement was performed in triplicate and all the experiments were carried out at 25 °C.

Viscosity measurement

Viscosity of ND 7 was measured using a Brook Field Viscometer (LV-II); the measurement was carried in triplicate.

Oxidative stability of all formulations during storage

Oxidative stability of ASEO before and after nanoemulsification and during storage was determined

by the primary oxidation products estimated measuring PV (peroxide value) according to AOCS official method Cd 8-53 (AOCS, 2003) and the secondary oxidation products assessed measuring p-AV (p-anisidine value) using AOCS Official Method Cd 18-90 (AOCS, 2009), with minor modifications. ND 7 and free ASEO (5% essential oil + 95% water) were stored in test tubes and then incubated in a hot air oven at 45°C for 12 days.

Determination of PV was calculated using the following equation:

$$PV = \frac{(S - B) \times N \times 1000}{W}$$

S: the volume of sodium thiosulfate used to titrate the ASEO,

B: the volume of sodium thiosulfate required for blank,

N: the normality of sodium thiosulfate solution used for titration,

W: the weight of ASEO.

Determination of p-AV was calculated using the following equation:

$$p - AV = \frac{(25) \times (1.2As - Ab)}{m}$$

As: the absorbance of test solution after reacting with p-anisidine,

Ab: the absorbance of the sample with addition of p-anisidine,

m: the mass of the ASEO containing in ND7.

Antimicrobial activity evaluation

Antimicrobial activity was determined by measuring Minimum Inhibitory Concentrations (MIC) of ASEO and ND 7.

Microorganisms

Antimicrobial activity was assessed as the inhibitory effect against the growth of three Gram-positive bacteria: Staphylococcus aureus ATCC 25923 (S. aureus), Bacillus subtilis ATCC 6633 (B. subtilis), and Listeria monocytogenes ATCC 7644 (L. monocytogenes); and three Gram-negative bacteria: Escherichia coli ATCC 25922 (E. coli), Salmonella typhimurium ATCC 6994 (S. typhimurium), and Pseudomonas aeruginosa ATCC 27853 (P. aeruginosa). All bacteria were supplied by Algeria Pasteur Institute.

Minimum Inhibitory Concentrations determination

Minimum Inhibitory Concentrations were determined by the agar dilution method approved by the National Committee for Clinical Laboratory Standards (NCCLS) and modified in 1999 (Hammer, Carson, Riley, 1999). Briefly, a series of two-fold dilutions of each essential oil, in concentrations ranging from 2% (v/v) to 0.03% (v/v), were prepared in Mueller Hinton agar with 0.5% (v/v) tween 20. Plates were dried at 35°C for 30min prior to inoculation with 1-2 ml spots containing approximately bacterial concentration of 10^4 CFU of each microorganism. Mueller Hinton agar, with only 0.5% (v/v) Tween-20, was used as a positive growth control. Inoculated plates were incubated at 35°C for 48h. Minimum inhibitory concentrations (MICs) were determined after 24h. The MICs were established as the lowest concentration of essential oil inhibiting the visible growth of each microorganism on the agar plate.

Statistical analysis

All experiments were performed in triplicates and results were tested for one-way analysis of variance using Fisher test (ANOVA, F-test). If the generated p-value is less than or equal to 0.05 ($p \leq 0.05$), it suggests that the observed result is considered statistically significant at the 5% significance level. On the other hand, if the p-value is greater than 0.05 ($p > 0.05$), it implies that the observed result is not statistically significant at the 5% significance level. In this case, there is insufficient

evidence to reject the null hypothesis, and any observed differences are likely due to random chance or sampling variability.

RESULTS AND DISCUSSION

Extraction and characterization of ASEO

The extraction yields were calculated as the weight of collected essential oil divided by the weight of dried material fed into the Clevenger apparatus. The average extraction yield of ASEO was of 2.72 ± 0.04 %.

The GC/MS analysis of the essential oil allowed the identification of 16 different compounds, accounting for a total of 94.78% of the essential oil's total weight. The major compound in the studied essential oil is trans-anethole, with a percentage of 86.02%. The detailed composition of the anise seed essential oil is provided in Table II, and the obtained GC/MS chromatogram is presented in Figure S1 of the supplemental material.

TABLE II - Composition of the Anise Seed Essential Oil

N°	Retention time (min)	Compounds	Kovats retention index	Percentage (%)
1	15,89	d-limonene	1026	0,12
2	20,24	Fenchone	1086	0,09
3	21,52	l-linalool	1096	0,49
4	28,37	Estragol	1196	1,88
5	31,71	Anisaldehyde	1242	0,06
6	31,38	Cis-anethol	1252	0,56
7	**35,46**	**Trans-anethol**	**1284**	**86,02**
8	38,01	α-Terpinene	1017	0,17
9	41,09	Anisylmethylketone	1382	0,19
10	44,76	Alpha-himachalene	1451	0,04
11	46,19	Gamma-himachalene	1482	2,09
12	46,24	Alpha-curcumene	1480	0,52
13	47,12	Alpha-zingiberene	1493	0,35
14	47,53	Beta-himachalene	1500	0,19
15	48,66	Beta-bisabolene	1507	0,06
16	66,68	Pseudoisoeugenyl 2-methylbutyrate	1842	1,95

Nanodispersion formulation, ASEO content and Laser Particle size analysis

Values of the ASEO content, the mean droplet size and polydispersity index of all formulations are given in Table III.

TABLE III - Laser Particle size analysis and ASEO content of nanoemulsion formulations

Formulations codes	Essential Oil Content (%)	Mean droplet size (nm)	Polydispersity index
ND 1	4,80 ± 0.04	17.83 ± 1.31	0.29 ± 0.03
ND 2	4,85 ± 0.07	18.2 ± 1.45	0.33 ± 0.03
ND 3	4,91 ± 0.05	19.02 ± 0.97	0.37 ± 0.03
ND 4	4,82 ± 0.05	19.87 ± 1.81	0.37 ± 0.03
ND 5	4,88 ± 0.04	17.17 ± 0.78	0.31 ± 0.03
ND 6	4,76 ± 0.04	17.23 ± 0.99	0.37 ± 0.03
ND 7	4,86 ± 0.06	19.02 ± 1.31	0.41 ± 0.03
ND 8	4,86 ± 0.03	19.14 ± 1.62	0.39 ± 0.03
ND 9	4,87 ± 0.08	18.82 ± 1.23	0.14 ± 0.03
ND 10	4,90 ± 0.05	19.68 ± 1.07	0.16 ± 0.03
ND 11	4,85 ± 0.06	20.84 ± 1.95	0.20 ± 0.03
ND 12	4,85 ± 0.03	21.14 ± 2.02	0.19 ± 0.03
ND 13	4,87 ± 0.07	18.13 ± 1.32	0.20 ± 0.02
ND 14	4,85 ± 0.07	18.46 ± 1.03	0.21 ± 0.02
ND 15	4,86 ± 0.04	19.32 ±1.41	0.29 ± 0.03
ND 16	4,88 ± 0.05	20.67 ± 1.07	0.24 ± 0.03

Overall, the concentration of essential oil in the various formulations is slightly below 5%, ranging from 4,76 ± 0.04% (ND6) to 4,91 ± 0.05% (ND3). This observed reduction is reasonable, as it can be attributed to the volatility of the essential oil, which is exacerbated by the different stages of the manufacturing process. Notably, during ultrasonic homogenization, the heating of the system facilitates the evaporation of volatile compounds.

The mean droplet size ranged from 17.17 ± 0.78 nm (ND5) to 20.84 ± 1.95 nm (ND 11), affirming the positive physical stabilizing effect of

chitosan/polysorbate 80 surfactants combination to completely coat the ASEO nanoemulsion and prevent it from disintegrating into large particles. It is worth mentioning that other researchers have produced ASEO nanoemulsions with larger droplet sizes compared to the current work. For example, (Topuz *et al*., 2016) synthesized ASEO nanoemulsions with smaller mean diameter ranging from 117.2 to 275.7 nm containing Neobee 1053 medium-chain triacylglycerol at different ratios. Additionally, another formulation composed of 14% (v/v) anise essential oil, 3% (v/v) ethanol, and Tween 80 (Hashem *et al*., 2018) resulted in ASEO nanoemulsions with a mean diameter of 198.9 nm. More recently, (Ghazy *et al*., 2021) synthesized anise extract nanoparticles using an ultrasound-assisted method and 5% Tween 80 with an average droplet size of 440 nm.

The polydispersity indexes of nanoemulsions were < 0.41, suggesting that all prepared emulsions have a relatively narrow range of size distribution and can be considered as nanoemulsions with a monodispersity. Polydispersity indexes ≥ 0.5 refer to a broad distribution (Patravale, Date, Kulkarni, 2004). ND 7 formulation presented significantly ($p < 0.05$) the highest polydispersity index 0.41 ± 0.03 with 19.02 ± 1.31 nm mean droplet size. The significant change of ND7 macroscopic aspect, before and after ultrasonication, and the schematic distribution of chitosan positive charges in the surface of ASEO droplet are presented in Figure 1A and 1B respectively.

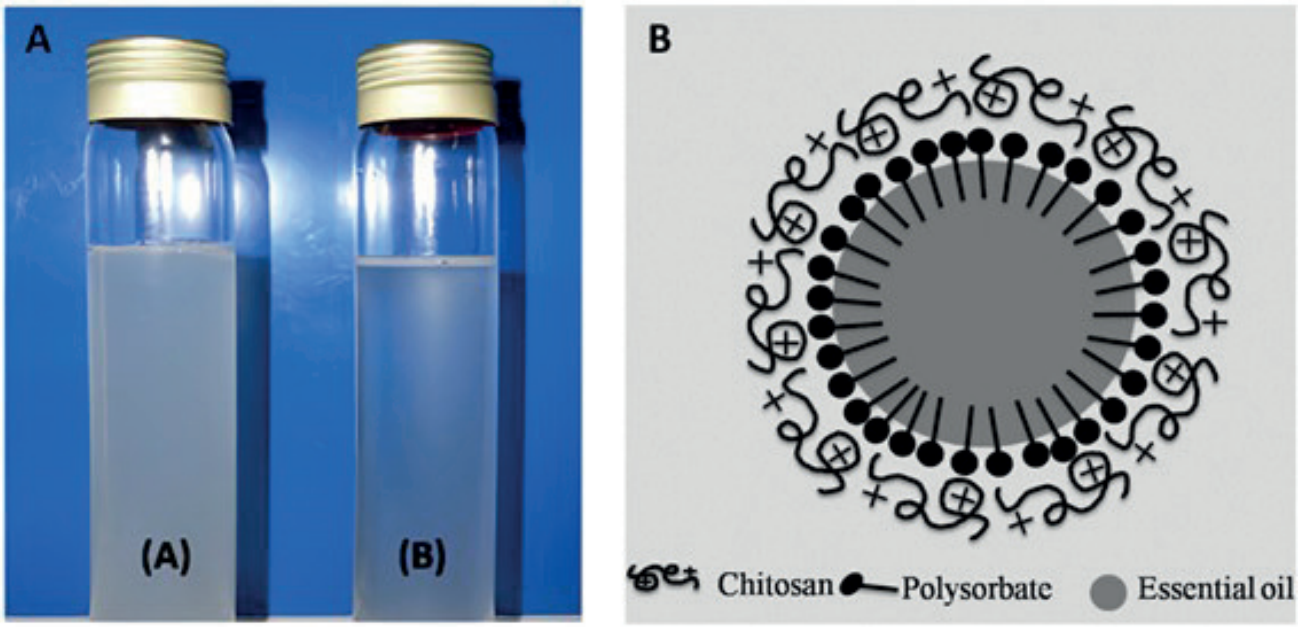

FIGURE 1 - Characteristics of ND 7: A. Photography (A) before and (B) after ultrasonication; B. Schematic distribution of chitosan positive charges on the surface of ASEO droplet.

Experimental design

Experimental data were analyzed by the software MODDE Pro 13 in order to find a mathematical relation between the factors (X1, X2, X3, X4) and the responses (Y1 and Y2).

All coefficients of the mathematical models, their standard errors and respective p-values estimated by multiple linear regression (MLR), and analysis of the variance (ANOVA) tools are given in Table IV. When the coefficients of independent factors are preceded by a negative sign, it indicates the increase of the response when the given factors are decreased. Conversely, the positive effect of the independent factors on the observed replies was demonstrated by the positive sign for the coefficients. Based on the p-values that determine the significance of the coefficients, it can be concluded that all the independent factors had a significant impact

on the mean droplet size ($p < 0.05$) while only three independent factors (X2, X3 and X4) had a significant impact on the polydispersity index ($p < 0.05$). Finally, Table IV also presents indicative parameters of the quality adjustment and prediction models in response surface, R^2 values of Y1 and Y2 are 0.975 and 0.995 respectively, and adjusted R^2 of Y1 and Y2 are 0.927 and 0.985 respectively. Prediction Q^2 of Y1 and Y2 are 0.746 and 0.950 respectively. The goodness of fit R^2 and the accuracy of prediction Q^2 values confirmed the high significance of the results.

TABLE IV - Coefficients of the mathematical models and their standard errors and p-values

	Mean droplet size (Y1)			Polydispersity index (Y2)		
	Coefficients	Standard errors (±)	p-value	Coefficients	Standard errors (±)	p-value
Constant	19,0394	0,0813275	2,6986e-11*	0,279375	0,00269548	1,58532e-09*
Tween (X1)	-0,270624	0,0813275	0,0208341*	-0,0031249	0,00269548	0,298668
Chito (X2)	-0,838125	0,0813275	0,00014794*	-0,028125	0,00269548	0,000139382*
Time (X3)	-0,385625	0,0813275	0,0051426*	0,023125	0,00269548	0,000354691*
Ampli (X4)	-0,593126	0,0813275	0,00075862*	0,075625	0,00269548	1,07713e-06*
Tween*Chito	0,056875	0,0813275	0,515532	-0,013125	0,00269548	0,00459587*
Tween*Time	0,0268745	0,0813275	0,754458	0,003125	0,00269548	0,298667
Tween*Ampli	0,0843751	0,0813275	0,34706	-0,0068750	0,00269548	0,0512309
Chito*Time	-0,0456258	0,0813275	0,598998	-0,0018750	0,00269548	0,517666
Chito*Ampli	0,0218751	0,0813275	0,798694	-0,001875	0,00269548	0,517672
Time*Ampli	0,101875	0,0813275	0,265727	-0,0081249	0,00269548	0,0296094*
R^2	0,975			0,995		
Adjusted R^2	0,926			0,985		
Q^2	0,746			0,950		

* indicates the model significance with $p < 0.05$

Effect of factors on mean droplet size (Y1)

The relationship between all the studied factors and mean droplet size (responses Y1) could be outlined by displaying the loading plot named "iso-response" curves shown in Figure 2.

From the obtained graphics (See Figure 2) and Scaled and Centered Coefficients for mean droplet size shown in Figure 3, the gradual decreases of all factors increases intensely up to the mean droplet size on nanoemulsion. Effect of factors on polydispersity index (Y2)

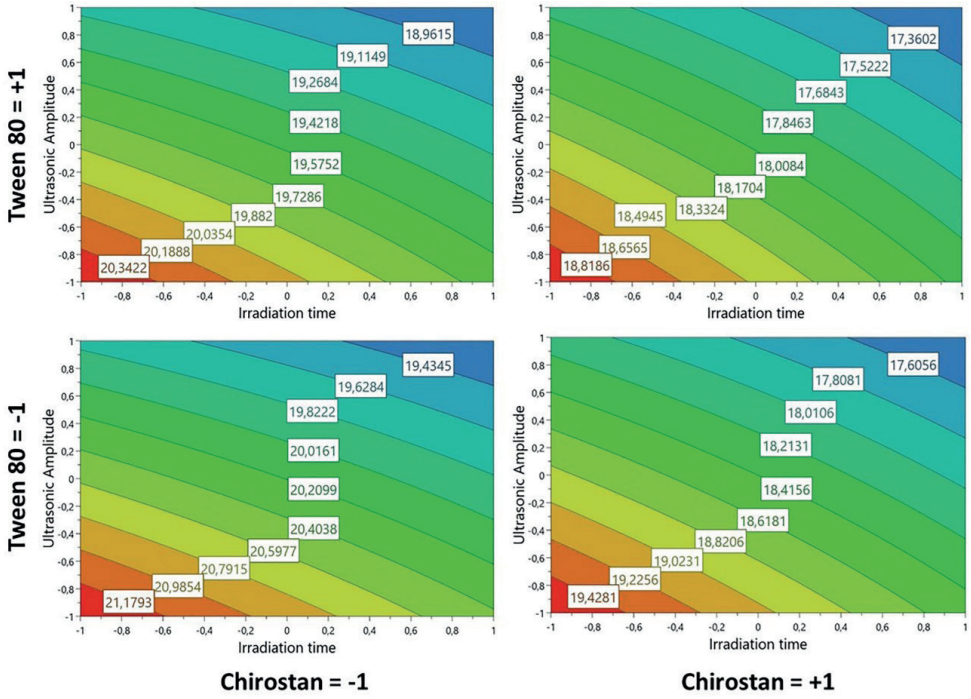

FIGURE 2 - Contour plot for mean droplet size.

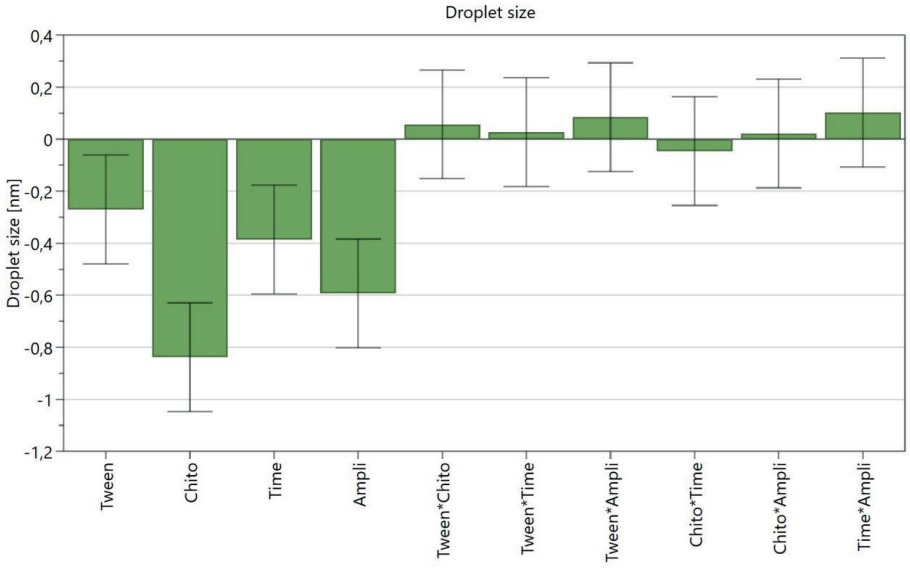

FIGURE 3 - Scaled and Centered Coefficients for mean droplet size.

Effect of factors on polydispersity index (Y2)

The relationship between all factors and polydispersity index (responses Y2) could be analysed by displaying the loading "iso-response" curves shown in Figure 4.

From the graphs obtained (See Figure 4) and the coefficients for polydispersity index shown in Figure 5, the gradual increases of X3 (irradiation time) and X4 (ultrasonic amplitude) increases dramatically up to the polydispersity index on nanoemulsion. On the other hand, when the factors X1 (Tween 80 content) and X2 (Chitosan content) increase, the polydispersity index of nanoemulsion is decreased; however, the negative influence of X2 is bigger than that of X1, which has practically no influence.

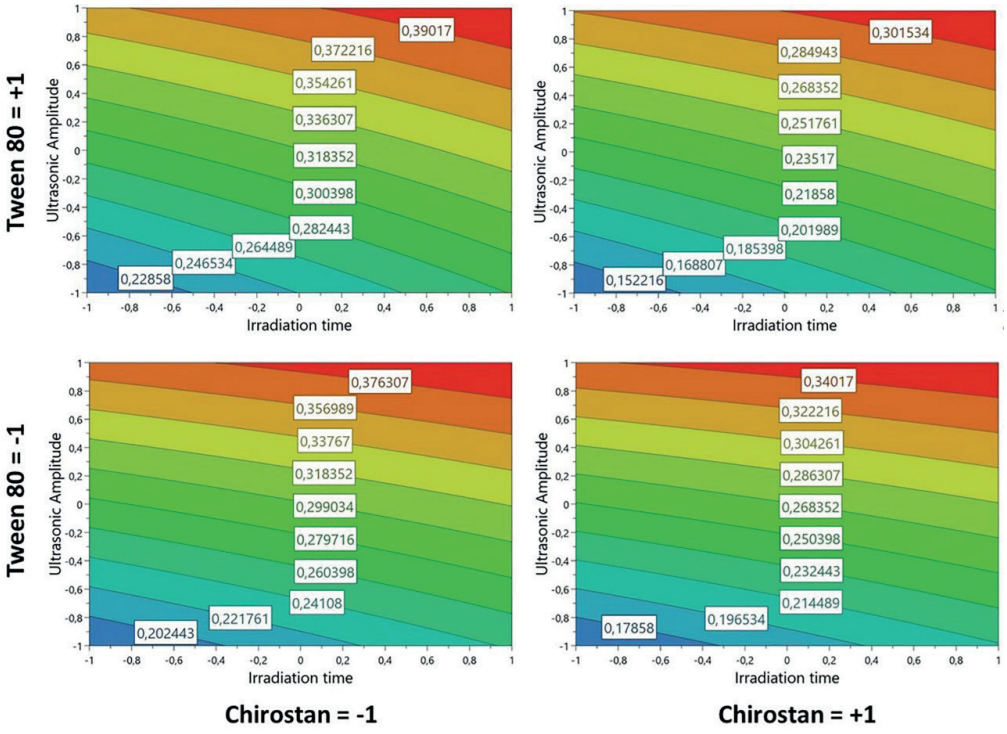

FIGURE 4 - Contour plot for polydispersity index.

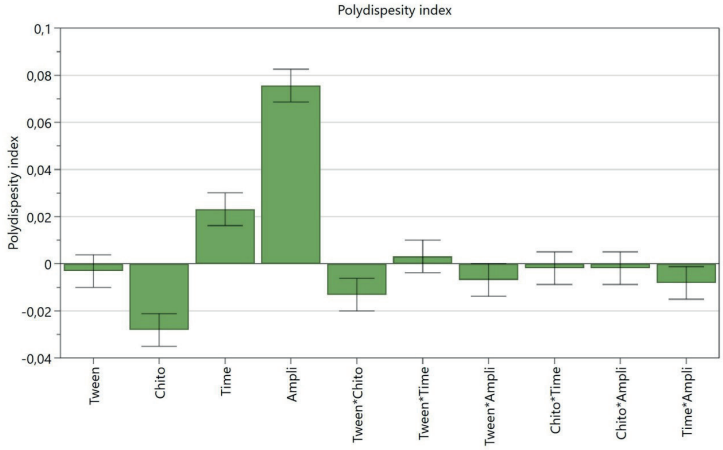

FIGURE 5 - Scaled and Centered Coefficients for polydispersity index.

Zeta potential analysis

The zeta potential of ND 7 was 31.42 ± 2.97 mV at 25 °C as a result of the positively charged chitosan molecules coated on the surface of ASEO droplet.

Viscosity measurement

The Viscosity of ND 7 was 104 ± 13.01 cP at 25 °C due to the gelifiant power and length chains of the chitosan macromolecules in colloidal form in the aqueous phase.

Stability study

Figure 6A and 6B present the changes in the PV (peroxide value) and in the p-AV (p-anisidine values) of ND7 nanoemulsion and free ASEO under storage for 12 days at 45°C respectively. Peroxide value of ASEO significantly increased on day 2 ($p \leq 0.05$), suggesting that the primary oxidation products started to appear in ASEO. The increase of PV for ND7 was significantly ($p \leq 0.05$) slow compared to free ASEO. Secondary oxidation products, as indicated by p-anisidine values, increased in the ASEO starting from day 2 ($p \leq 0.05$). The augmentation of secondary oxidation products in ASEO was significantly slow and slight when ASEO is nanodespersed in ND7 formulation.

In this method, peroxide value and p-anisidine values increased in the free ASEO due to temperature, oxygen, and water content (Turek, Stintzing, 2013). Nanodispersed ASEO in water stabilized by chitosan

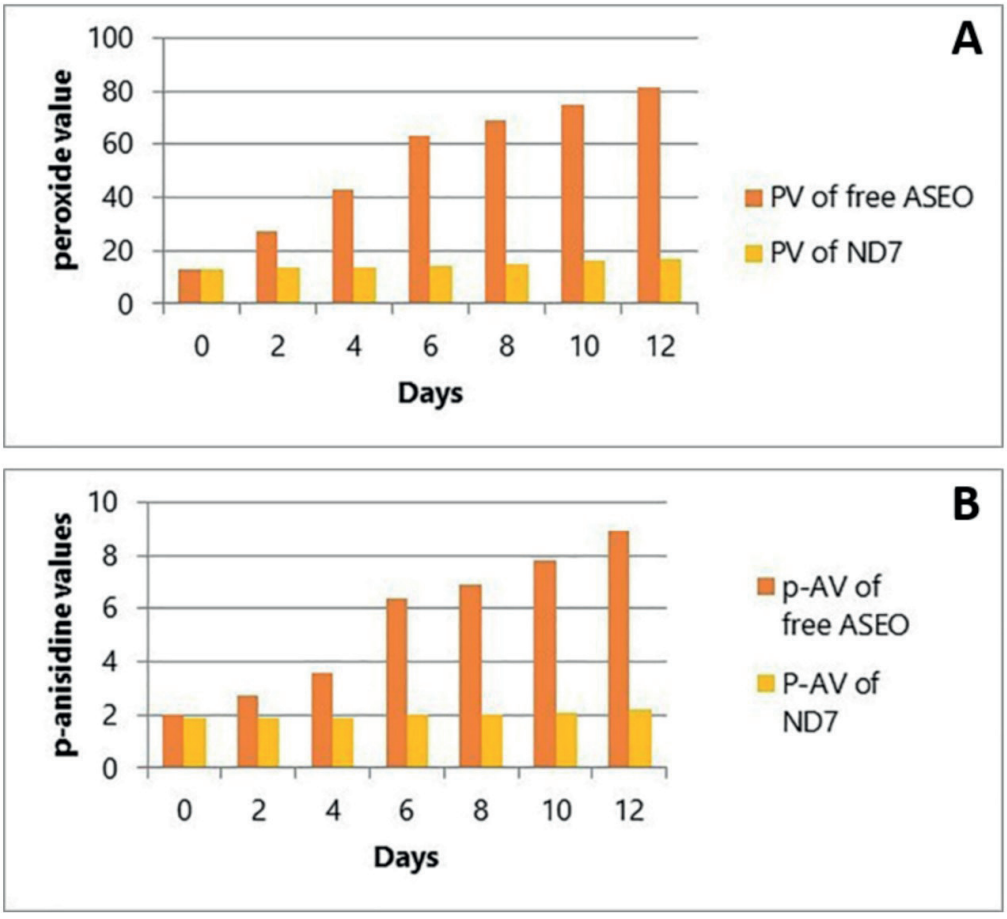

FIGURE 6 - Stability study of ND7 and free ASEO: A. Changes in the PV (peroxide value) of ND7 nanoemulsion and free ASEO under storage for 12 days at 45°C; B. Changes in the p-AV (p-anisidine values) of ND7 nanoemulsion and free ASEO under storage for 12 days at 45°C.

In this method, peroxide value and p-anisidine values increased in the free ASEO due to temperature, oxygen, and water content (Turek, Stintzing, 2013). Nanodispersed ASEO in water stabilized by chitosan and polysorbate 80 (ND7) presents good oxidative stability at (45°C), but the free ASEO presents formation of oxidation products which confirmed its degradation.

The major compound of ASEO is trans-anethole (Misharina, Polshkov, 2005); it was observed that trans-anethole had totally oxidized to anisaldehyde or isomerized to cis-anethole (See Figure 7) after 2 months of storage at room temperature under light, in sweet fennel oil.

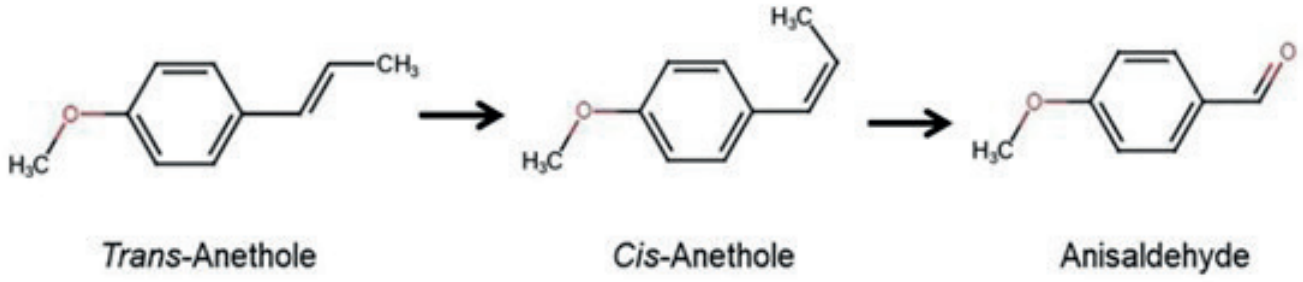

FIGURE 7 - Isomerization and oxidation products of trans-anethole detected in fennel oil.

When trans-anethole undergoes oxidation, the double bond in the molecule is converted into a carbonyl group, resulting in the formation of anisaldehyde.

Isomerization refers to the rearrangement of atoms within a molecule to form a different isomer. In the case of trans-anethole, it can isomerize to cis-anethole, which involves a change in the orientation of the substituents around the double bond. Isomerization reactions can occur spontaneously or can be catalyzed by heat, acid, or other suitable catalysts.

In our case, these chemical reactions accelerate due to the temperature dependence of the reactions rate as expressed by the Arrhenius equation (Atkins, 2002). Trans-anethole, the main constituent in fennel essential oil, was reported to be converted to cis-anethole, which is 10 to 12 times more toxic, when treated with high temperatures or UV rays (Braun, Franz, 1999). (Pfau, 1972) already described photo-chemically catalyzed intramolecular isomerization reactions such as cycloaddition or trans-cis conversions of various monoterpenoids. These reactions are initiated by the absorption of light energy by the molecule, which promotes electronic transitions and allows for structural rearrangements.

Cycloaddition reactions involve the formation of cyclic compounds through the concerted bonding of two or more reactant molecules. In the context of monoterpenoids, photochemical cycloaddition reactions can result in the formation of cyclic structures within the molecule itself. The specific types of cycloadditions that can occur depend on the structure and functional groups present in the monoterpenoid.

Trans-cis conversions refer to the isomerization of a double bond from the trans configuration to the cis configuration or vice versa. In the case of monoterpenoids, photochemical excitation can induce the isomerization of the double bond within the molecule, resulting in a change in the spatial arrangement of substituents around the double bond.

The occurrence and extent of these photochemically induced isomerization reactions depend on several factors, including the structure of the monoterpenoid,

the wavelength and intensity of the incident light, the presence of suitable catalysts or sensitizers, and the reaction conditions (such as temperature and solvent).

It is important to note that the specific reactions and mechanisms involved in the photochemically catalyzed intramolecular isomerization reactions of monoterpenoids can vary greatly depending on the individual compound and the conditions of the experiment. Each monoterpenoid may have its unique reactivity and photophysical properties, leading to different products and pathways upon photoexcitation.

Antimicrobial activity evaluation

The MICs of free ASEO and ND7 nanoemulsion achieved by the agar dilution method are presented in Table V.

TABLE V - Minimum inhibitory concentrations (MICs) of ASEO and ND7 (% v/v) against 6 different microorganisms

	Test Microorganisms (bacteria)					
	Gram-positive			Gram-negative		
	Staphylococcus aurous ATCC 25923	Bacillus subtilis ATCC 6633	Listeria monocytogenes ATCC 7644	Pseudomonas aeruginosa ATCC 27853	Escherichia coli ATCC 25922	Salmonella typhimurium ATCC 6994
MICs of Free ASEO	1	> 0.5	> 1	2	0.5	-
MICs of ND7	0.5	> 0.12	0.5	0.25	> 0.06	2

-: No antimicrobial activity was shown by agar dilution method.

It was observed that the Gram+ bacteria that exhibited the higher sensitivity to free ASEO, after its nanodispersion ND7, presented an even higher antibacterial activity. This antibacterial potential is even more important for Gram- bacteria than for Gram+ bacteria. ASEO inhibited all microorganisms except Salmonella typhimurium, but its nanodispersion presents MIC = 2% (v/v). The enhancement of the antimicrobial activity of the applied ASEO nanoemulsion comapred to free ASEO can be attributed to the size of the nanoemulsion which is smaller than the porosity of the bacterial membrane, allowing the penetration and delivery of bioactive substances (mainly trans-anethole in our case) into the bacteria to enhance its antibacterial activity. These results are in accordance with literature where studies have shown that nanoemulsions containing anise oil exhibit antimicrobial properties against a range of pathogens, including Gram+ and Gram- bacteria, yeast, and fungi (Abu Ali *et al*., 2021).

Essential oils nanoemulsions have gained attention as potential antimicrobial agents due to their improved stability, enhanced solubility, and increased bioavailability. The antimicrobial activity of essential oil nanoemulsions can be attributed to several mechanisms. Essential oil nanoemulsions can interact with microbial cell membranes, leading to membrane disruption. The nanoemulsion droplets can penetrate the lipid bilayer, causing destabilization and leakage of cellular contents. This disruption can interfere with essential functions of microbial cells, leading to their death or inhibition of growth.

Essential oils contain bioactive components, such

as terpenoids and phenolics, that present antioxidant properties. These compounds can generate reactive oxygen species (ROS) within microbial cells, causing oxidative stress. ROS can damage cellular components, including oxidation of DNA, peroxidation of lipids, and carbonylation of proteins leading to cell death or growth inhibition.

Essential oil nanoemulsions can interfere with microbial enzymes responsible for vital metabolic processes. The bioactive compounds in essential oils can inhibit the activity of enzymes involved in cellular respiration, energy production, and synthesis of essential molecules. By disrupting these enzymatic pathways, the nanoemulsions can disrupt microbial growth and survival. Essential oil nanoemulsions can influence gene expression in microbial cells. The bioactive compounds in essential oils can interact with microbial genetic material, leading to the upregulation or downregulation of specific genes. This modulation of gene expression can affect microbial survival, replication, and virulence.

It is important to note that the antimicrobial mechanisms of essential oil nanoemulsions can vary depending on the specific composition of the essential oil, the formulation of the nanoemulsion, the target microorganism, and the experimental conditions. Further research is ongoing to better understand and optimize the antimicrobial activity of essential oil nanoemulsions for various applications.

CONCLUSION

The novelty of the present work is to find optimal conditions through the screening process of all possible combinations of the studied factors for the preparation of nanoemulsion based essential oils. In our case, anise seeds essential oil, experimental design permitted to screen its droplet size and its polydispersity index. The oxidative stability of the prepared nanoemulsion conferred by the nanodispersed system stabilized by polysorbate 80 and chitosan mixture has significantly increased. However, the most interesting result is the behavior of nanoemulsion against bacteria; the enhancement of antibacterial activity against Gram- bacteria is bigger than Gram+ bacteria while the free essential oil presents the contrary. These significant results can be used like a reference for future works on essential oils nanodispersion preparation, sonication technique uses, chitosan/polysorbate 80 mixture uses, stability of bioactive substances, and enhancement of antimicrobial activity of natural antibiotics.

REFERENCES

Abu Ali OA, El-Naggar ME, Abdel-Aziz MS, Saleh DI, Abu-Saied MA, El-Sayed WA. Facile Synthesis of Natural Anise-Based Nanoemulsions and Their Antimicrobial Activity Polymers. 2021;13(12):2009.

Adams, RP. Identification of Essential Oil Components by Gas Chromatography-Mass Spectrometry (4th ed). Carol Stream, Illinois: Allured Publishing Corp. 2007.

AOCS, Official methods and recommended practices of the American Oil Chemists' Society. Method Cd 8-53. 6th Ed., Champaign: AOCS Press 2003:8-53.

AOCS, Official methods and recommended practices of the American Oil Chemists' Society. Method Cd 18-90. 6th Ed., Champaign: AOCS Press. 2009:18-90.

Atkins PW. Kurzlehrbuch Physikalische Chemie (3rd ed). Weinheim: Wiley-VCH; 2002.

Box GPE, Hunter WG, Hunter JS. Statistics for Experimenters: an Introduction to Design, Data Analysis, and Model Building (2nd ed). New York: John Wiley and sons. 1978:1-14,173-222,363-385.

Braun M, Franz G. Quality criteria of bitter fennel oil in the German Pharmacopoeia. Pharm Pharmacol Lett. 1999;9:48-51.

British Pharmacopoeia Commission. British Pharmacopoeia; The Stationery Office: London, UK. 2003; Appendix 9; Volume IV, p. A238.

Canselier JP, Delmas H, Wilhelm AM, Abismail B. Ultrasound emulsification—An overview. J Dispers

Sci. Technol. 2002;23:333-349.

Draz KA, Tabikha RM, Eldosouky MI, Darwish AA, Abdelnasser M. Biotoxicity of essential oils and their nano-emulsions against the coleopteran stored product insect pests Sitophilus oryzae L. and Tribolium castaneum herbst. Int J Pest Manag. 2022;1-15.

Ghazy OA, Fouad MT, Saleh HH, Kholif AE, Morsy TA. Ultrasound-assisted preparation of anise extract nanoemulsion and its bioactivity against different pathogenic bacteria. Food Chem. 2021;341:128259.

Gumiero VC, Da Rocha Filho PA. Babassu nanoemulsions have physical and chemical stability. J Dispers Sci Technol. 2012;33(11):1569-1573.

Hammer KA, Carson CF, Riley TV. Antimicrobial activity of essential oils and other plant extracts. J Appl Microbiol. 1999;86(6):985-990.

Hashem AS, Awadalla SS, Zayed GM, Maggi F, Benelli G. Pimpinella anisum essential oil nanoemulsions against Tribolium castaneum-insecticidal activity and mode of action. Environ Sci Pollut Res. 2018;25:18802-18812.

Hashem AS, Ramadan MM, Abdel-Hady AAA, Sut S, Maggi F, Dall'Acqua S. Pimpinella anisum Essential Oil Nanoemulsion Toxicity against Tribolium castaneum? Shedding Light on Its Interactions with Aspartate Aminotransferase and Alanine Aminotransferase by Molecular Docking. Molecules. 2020;25(20):4841.

Leong TSH, Wooster TJ, Kentish SE, Ashokkumar M. Minimising oil droplet size using ultrasonic emulsification. Ultrason Sonochem. 2009;16(6):721-727.

Misharina, TA, Polshkov AN. Antioxidant properties of essential oils: autoxidation of essential oils from laurel and fennel and of their mixtures with essential oil from coriander. Appl Biochem Microbiol. 2005;41(6):610-618.

Nait Bachir Y, Nait Bachir R, Hadj-Ziane-Zafour A. Nanodispersions stabilized by β-cyclodextrin nanosponges: application for simultaneous enhancement of bioactivity and stability of sage essential oil. Drug Dev Ind Pharm. 2018;45(2):333-347.

Nait Bachir Y, Medjkane M, Benaoudj F, Sahraoui N, Hadj-Ziane A. Formulation of β-Cyclodextrin Nanosponges by Polycondensation Method: Application for Natural Drugs Delivery and Preservation. J Mater Process Environ. 2017;5(1):80-85.

Nait Bachir Y, M. Formulation of stable microcapsules suspensions content Salvia officinalis extract for its antioxidant activity preservation. J Food Process Preserv. 2018;42(2):e13446.

Nait Bachir Y, Sahraoui N, Cheurfa Z, Hadj-ziane A. Formulation of a natural nanosystem based on β-cyclodextrin/arginine/xanthan to increase antifungal activity of Salvia officinalis essential oil from Algeria (Bejaïa, Kalaa n'Ath Abas). J Res Pharm. 2022;26(3):581-597.

Patravale V, Date AA, Kulkarni R. Nanosuspensions: A promising drug delivery strategy. J Pharm Pharmacol. 2004;56(7):827–840.

Pfau M. Photochemistry in the field of monoterpenes and related compounds. Flavour Ind. 1972;3:89-103.

Puglia C, Rizza L, Drechsler M, Bonina F. Nanoemulsions as vehicles for topical administration of glycyrrhetic acid: characterization and in vitro and in vivo evaluation. Drug Deliv. 2010;17(3):123-129.

Sakulku U, Nuchuchua O, Uawongyart N, Puttipipatkhachorn S, Soottitantawat A, Ruktanonchai U. Characterization and mosquito repellent activity of citronella oil nanoemulsion. Int J Pharm. 2009;372(1-2):105-111.

Salfinger Y, Tortorello ML (Eds.). Compendium of methods for the microbiological examination of foods. Washington, DC: American Public Health Association; 2015.

Shaaban HA, El-Ghorab AH, Shibamoto T. Bioactivity of essential oils and their volatile aroma components. J Essent Oil Res. 2012;24(2):203-212.

Shojaii A, Abdollahi Fard M. Review of Pharmacological Properties and Chemical Constituents of Pimpinella anisum. ISRN Pharm. 2012;2012:510795.

Slamani M, Zaouadi N, Gharbi D, Nait Bachir Y, Hadj Ziane-Zafour A. Formulation of an oral emulsion for the delivery of active substances contained in Atriplex halimus L. leaves. J Fundam Appl Sci. 2020;12(1S):35-48.

Topuz OK, Özvural EB, Zhao Q, Huang Q, Chikindas M, Gölükçü M. Physical and antimicrobial properties of anise oil loaded nanoemulsions on the survival of foodborne pathogens. Food Chem. 2016;203:117-123.

Turek C, Stintzing, FC. Stability of essential oils: a review. Compr Rev Food Sci Food Saf. 2013;12(1):40-53.

Wooster TJ, Golding M, Sanguansri P. Impact of oil type on nanoemulsion formation and Ostwald ripening stability. Langmuir. 2008;24(22):12758-12765.

Received for publication on March 29th, 2024
Accepted for publication on October 3rd, 2024
Associated Editor: Ruy Beck

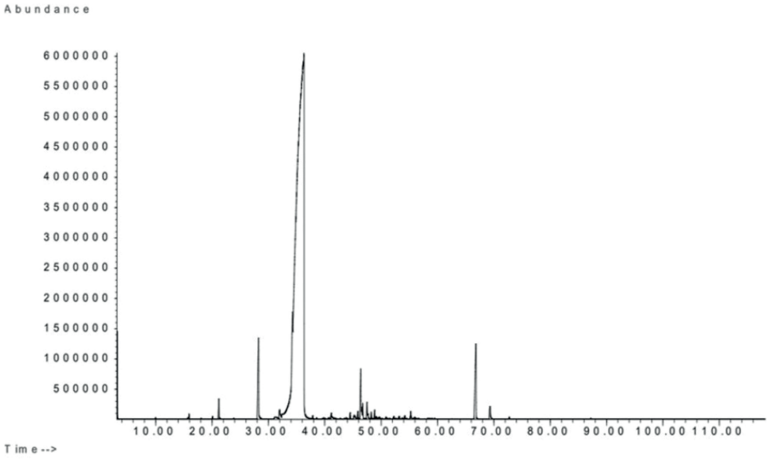

FIGURE S1 - GC/MS Chromatogram of Anise Seed Essential Oil.